Vol 18 No 11, November 2009
1674-1056/2009/18(11)/4797-10

Chinese Physics B

© 2009 Chin. Phys. Soc.
and IOP Publishing Ltd

Apparent diffusion behaviour of intermolecular double-quantum coherence modulated by a distant dipolar field in solution NMR*

Shen Gui-Ping(沈桂平)[a], Cai Cong-Bo(蔡聪波)[b],
Cai Shu-Hui(蔡淑惠)[a]†, and Chen Zhong(陈 忠)[a]

[a] *Department of Physics, Fujian Key Laboratory of Plasma and Magnetic Resonance, Xiamen University, Xiamen* 361005, *China*

[b] *Department of Communications Engineering, Xiamen University, Xiamen* 361005, *China*

(Received 15 April 2009; revised manuscript received 11 May 2009)

A modified correlated spectroscopy (COSY) revamped with asymmetric Z-gradient echo detection sequence was designed to investigate the influence of diffusion behaviour on intermolecular double-quantum coherence signal attenuation during the pre-acquisition period. Theoretical formulas were deduced and experimental measurements and simulations were performed. It is found that the diffusion behaviour of intermolecular double-quantum coherence in the pre-acquisition period may be different from that of conventional single-quantum coherence, depending on the relative orientation of diffusion weighting gradients to coherence selection gradients. When the orientation of the diffusion weighting gradients is parallel or anti-parallel to the orientation of the coherence selection gradients, the diffusion is modulated by the distant dipolar field. This study is helpful for understanding the signal properties in intermolecular double-quantum coherence magnetic resonance imaging.

Keywords: nuclear magnetic resonance, intermolecular double-quantum coherences, distant dipolar field, diffusion

PACC: 3240, 7660, 6610

1. Introduction

In solution nuclear magnetic resonance (NMR), when a two-pulse sequence separated by a time interval is applied to a highly polarized spin system, multiple spin echoes (MSEs) or intermolecular multiple-quantum coherences (iMQCs) can be observed in the presence of magnetic field gradients.[1,2] Nowadays, the pulse sequences for creating MSEs or iMQCs are mostly based on the correlated spectroscopy (COSY) revamped with asymmetric Z-gradient echo detection (CRAZED) sequence. MSEs and iMQCs can be described by using either the quantum mechanical density matrix treatment or the classical dipolar field treatment.[2,3] Both treatments have led to the same quantitative predictions for all the NMR signals derived from the CRAZED and similar sequences.[4−6] Since iMQCs have intrinsic properties different from conventional single-quantum coherences (SQCs) or intramolecular MQCs,[7−11] they have found wide applications in NMR spectroscopy and magnetic resonance imaging (MRI).[12−17] For example, the unique diffusion behaviours of iMQCs have been utilized in diffusion-weighted MRI to provide new information and novel contrast for improving the detection of water molecules associated with ordered structures in soft tissues.[15,18−21] Since diffusion-weighted gradients (DWGs) applied during the evolution period or the pre-acquisition period in iMQC pulse sequences result in different physical processes, the corresponding apparent diffusion coefficients may be different. To the best of our knowledge, no quantitative or even qualitative discussion on the diffusion properties of iMQCs during the pre-acquisition period has been presented to date.[6,7,22−28]

In this work, we will report our investigation on the intermolecular double-quantum coherence (iDQC) diffusion behaviour during the pre-acquisition period. A modified two-pulse CRAZED sequence was proposed for this investigation, where the signal attenuation was weighted by diffusion in the pre-acquisition period. Theoretical expressions were deduced, and

*Project supported by the National Natural Science Foundation of China (Grant No 10875101) and the Natural Science Foundation of Fujian Province, China (Grant No 2008J0028).

†E-mail: shcai@xmu.edu.cn

experiments and simulations based on the nonlinear Bloch equations were performed.[29] Theoretical, experimental and simulated results show that the apparent diffusion coefficient is correlated with the spatial modulation of the distant dipolar field (DDF), and different orientation of DWGs relative to the coherence selection gradients (CSGs) results in different apparent diffusion rates.

2. Theoretical formalism

The iMQC signal intensity in the CRAZED experiments is influenced by molecular diffusion,[22] dipolar correlation distance,[14] radiation damping,[30] background field inhomogeneity,[31] spin relaxation,[32] and so on. All these factors may directly impose effects on the precision and accuracy of diffusion measurement. Although a quantitative description of the signal attenuation caused by all these factors is difficult, it is possible to design some pulse sequences where the relative signal attenuation is only dominated by the diffusion effect. In this paper, to quantitatively investigate the iDQC apparent diffusion behaviour during the pre-acquisition period, a modified CRAZED pulse sequence shown in Fig.1

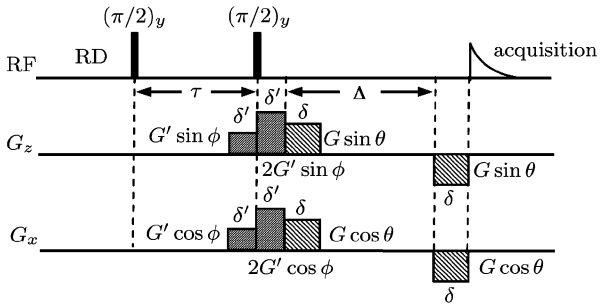


Fig.1. Modified CRAZED pulse sequence for studying iDQC diffusion behaviour in the pre-acquisition period.

is proposed. The first pair of gradient pulses with duration δ' and magnitude G' or $2G'$ are used for the iDQC selection. The second pair of gradient pulses with duration δ, magnitude G and interval Δ are used for diffusion weighting during the pre-acquisition period. They are along the z or x direction, depending on the ϕ and θ angles respectively, where ϕ is the angle between the first CSG and x direction and θ is the angle between the first DWG and x direction. The radiation damping effect during the short evolution period τ is suppressed by the first CSG before the second RF pulse. The bipolar pulse field gradients (PFGs) in the pre-acquisition period not only act as DWGs, but also help to suppress the radiation damping effect. For all experiments performed in this study, the radiation damping effects are further suppressed by deliberately detuning the probe.

An isolated spin –1/2 system with unrestricted isotropic diffusion has been considered. The CSGs are applied along the z direction, i.e. $\phi = \pi/2$. For the pulse sequence shown in Fig.1, the variation of magnetization with time can be described by the Bloch equations. When radiation damping and background field inhomogeneity are ignored, we have[1,22]

$$\frac{\mathrm{d}M_z(z,t)}{\mathrm{d}t} = -\frac{M_z(z,t)-M_0}{T_1} + D_{\mathrm{T}}\left(\frac{\partial^2}{\partial x^2}+\frac{\partial^2}{\partial z^2}\right)M_z(z,t)\ , \tag{1a}$$

and

$$\frac{\mathrm{d}M_+(z,t)}{\mathrm{d}t} = \gamma\{M_+(z,t)\times[B_0(z)+B_d(z)]\} - \frac{M_+(z,t)}{T_2} + D_{\mathrm{T}}\left(\frac{\partial^2}{\partial x^2}+\frac{\partial^2}{\partial z^2}\right)M_+(z,t), \tag{1b}$$

where γ is the gyromagnetic ratio of the investigated nuclei. M_0 is the equilibrium magnetization, and $M_z(z,t)$ and $M_+(z,t) = M_x + \mathrm{i}\,M_y$ are local longitudinal and transverse magnetization components, respectively. T_1 and T_2 represent the longitudinal and transverse relaxation times, respectively, and D_{T} is the conventional molecular translational diffusion coefficient. $B_0(z)$ is the external static magnetic field, and $B_{\mathrm{d}}(z)$ is the DDF. In order to simplify the calculations, the durations of RF pulses are assumed to be short enough to permit the neglect of relaxation and diffusion effects during their actions.

2.1. iMQC model

In Fig.1, all the RF pulses are not selective and are applied along the y axis of the rotating frame. The gradient pulses can be made much stronger than the background field gradients, so the latter will be neglected in the following analysis. Before the first $(\pi/2)_y$ RF pulse, the equilibrium magnetization M_0 is aligned along the z direction. Just after the first

gradient pulse, i.e. after the time τ following the initial RF pulse, the magnetization becomes

$$M_+\left(z,\tau^+\right) = M_0 \mathrm{e}^{-\tau/T_2}\mathrm{e}^{\mathrm{i}\,\phi_{z1}}\mathrm{e}^{-b_1 D_\mathrm{T}},$$
$$M_z\left(z,\tau^+\right) = M_0\left(1-\mathrm{e}^{-\tau/T_1}\right). \quad (2)$$

The superscript + (or – in the following text) indicates the moment immediately after (or before) certain event (e.g. after an evolution time τ). The phase shift is $\phi_{z1} = kz$, with $k = \gamma G'\delta'$. The $\mathrm{e}^{-b_1 D_\mathrm{T}}$ represents diffusion attenuation caused by the first CSG pulse before the second RF pulse, where

$$b_1 = \gamma^2 G'^2 \delta'^3/3$$

is the diffusion weighting factor generated by the first CSG pulse.[22] Immediately after the second RF pulse the transverse and longitudinal magnetization components turn into

$$M_+\left(z,\tau,\delta'^-\right) = M_0\left[\left(1-\mathrm{e}^{-\tau/T_1}\right)+\frac{1}{2}\left(\mathrm{e}^{\mathrm{i}\,\varphi_{z1}}-\mathrm{e}^{-\mathrm{i}\,\varphi_{z1}}\right)\mathrm{e}^{-\tau/T_2}\mathrm{e}^{-b_1 D_\mathrm{T}}\right],$$
$$M_z\left(z,\tau,\delta'^-\right) = -\frac{1}{2}M_0\left(\mathrm{e}^{\mathrm{i}\,\varphi_{z1}}+\mathrm{e}^{-\mathrm{i}\,\varphi_{z1}}\right)\mathrm{e}^{-\tau/T_2}\mathrm{e}^{-b_1 D_\mathrm{T}}. \quad (3)$$

From Eq.(1), it is obvious that the evolution of the local longitudinal magnetization component is only affected by the longitudinal relaxation and molecular diffusion. Therefore, it is independent of the evolution of the transverse magnetization component from now on.

$$M_z\left(z,\tau,t_2\right) = -\frac{1}{2}M_0\left(\mathrm{e}^{\mathrm{i}\,\varphi_{z1}}+\mathrm{e}^{-\mathrm{i}\,\varphi_{z1}}\right)\mathrm{e}^{-\tau/T_2}\mathrm{e}^{-b_1 D_\mathrm{T}}\mathrm{e}^{-\left(k^2 D_\mathrm{T}+1/T_1\right)t_2}+M_0\left(1-\mathrm{e}^{-t_2/T_1}\right). \quad (4)$$

As a consequence, a spatially modulated DDF, B_d, is given by[32]

$$B_\mathrm{d}(z,\tau,t_2) = -\mu_0 M_0 \cos\varphi_{z1}\mathrm{e}^{-\tau/T_2}\mathrm{e}^{-b_1 D_\mathrm{T}}\mathrm{e}^{-\left(k^2 D_\mathrm{T}+1/T_1\right)t_2}, \quad (5)$$

where μ_0 is vacuum magnetic permeability. The DDF contributes a rotation of the transverse magnetization around z at the angular velocity $-\gamma B_\mathrm{d}$ which depends on z and t_2. It will be convenient for further calculations to express the rotation angle accumulated from $t_2 = 0$ in the form of $\xi\left(t_2\right)\cos\phi_{z1}$, where $\xi\left(t_2\right)$ is easily evaluated from Eq.(5),

$$\xi(t_2) = \frac{\gamma\mu_0 M_0 \mathrm{e}^{-\tau/T_2}\mathrm{e}^{-b_1 D_\mathrm{T}}\left[1-\mathrm{e}^{-\left(k^2 D_\mathrm{T}+1/T_1\right)t_2}\right]}{k^2 D_\mathrm{T}+1/T_1}. \quad (6)$$

The dipolar field gradient (DFG) generated by the DDF is then given by

$$G_\mathrm{d}(z,\tau,t_2) = \frac{\partial B_\mathrm{d}\left(z\right)}{\partial z} = \gamma G'\delta'\mu_0 M_0 \sin\varphi_{z1}\mathrm{e}^{-\tau/T_2}\mathrm{e}^{-b_1 D_\mathrm{T}}\mathrm{e}^{-\left(k^2 D_\mathrm{T}+1/T_1\right)t_2}. \quad (7)$$

After integration over the sample, the effective DFG can be obtained from Eq.(7),

$$G_\mathrm{d}\left(\tau,t_2\right) = \int_0^L \gamma G'\delta' A_0\mu_0 M_0 \sin\varphi_{z1}\mathrm{d}z = A_0\mu_0 M_0\left[1-\cos\left(\gamma G'\delta' L\right)\right], \quad (8)$$

where L is the effective length of the sample, $A_0 = \mathrm{e}^{-\tau/T_2}\mathrm{e}^{-b_1 D_\mathrm{T}}\mathrm{e}^{-\left(k^2 D_\mathrm{T}+1/T_1\right)t_2}$ is the amplitude factor. As shown in Eq.(5), the DDF will remain stable for a long period since it dissipates slowly under the combined influence of nuclear spin lattice relaxation and molecular diffusion.[33] Therefore, for simplicity, we will neglect the dissipation of the DFG during the pre-acquisition period and detection period in the following discussion.

After the second RF pulse, the transverse magnetization evolves under the combined effects of transverse relaxation, the second CSG pulse, DWGs, and DDF, hence

$$M_+(z,\tau,t_2) = M_0\left[\left(1-\mathrm{e}^{-\tau/T_1}\right)+\frac{1}{2}\left(\mathrm{e}^{\mathrm{i}\,\varphi_{z1}}-\mathrm{e}^{-\mathrm{i}\,\varphi_{z1}}\right)\mathrm{e}^{-\tau/T_2}\mathrm{e}^{-b_1 D_\mathrm{T}}\right]$$
$$\times\,\mathrm{e}^{\mathrm{i}\,n\varphi_{z1}}\mathrm{e}^{\mathrm{i}\,\xi(t_2)\cos\varphi_{z1}}\mathrm{e}^{-t_2/T_2}\mathrm{e}^{-(b_2+b_3)D_\mathrm{T}} f(G',\delta',n), \quad (9)$$

where $f(G',\delta',n)=\mathrm{e}^{-k^2t_2D_\mathrm{T}}\mathrm{e}^{-\left(n\gamma G'\delta'\right)^2\left(\delta'/3+t_2\right)D_\mathrm{T}}$ is a complex function representing the diffusion attenuation caused by the CSGs located immediately before and after the second RF pulse, b_2 and b_3 are the diffusion weighting factors caused by the DWGs and the DFG respectively. Detailed expressions for these factors will be given in the next subsection.

Equation (9) can be transformed to the following expression by using the Bessel function expansion,

$$M_+(z,\tau,t_2)=M_0\left[\left(1-\mathrm{e}^{-\tau/T_1}\right)+\frac{1}{2}\left(\mathrm{e}^{\mathrm{i}\,\varphi_{z1}}-\mathrm{e}^{-\mathrm{i}\,\varphi_{z1}}\right)\mathrm{e}^{-\tau/T_2}\mathrm{e}^{-b_1D_\mathrm{T}}\right]\mathrm{e}^{-t_2/T_2}\mathrm{e}^{\mathrm{i}\,n\varphi_{z1}}\mathrm{e}^{-(b_2+b_3)D_\mathrm{T}}$$
$$\times f(G',\delta',n)\sum_{m=-\infty}^{\infty}\mathrm{i}^m\mathrm{J}_m\left(\xi\right)\mathrm{e}^{\mathrm{i}\,m\varphi_{z1}},\tag{10}$$

where J_m is the m-order Bessel function. Since $\tau\ll T_1$, the first term in Eq.(10) can be negelected and Eq.(10) can be changed into

$$M_+(z,\tau,t_2)=\frac{M_0}{2}\mathrm{e}^{-(\tau+t_2)/T_2}\mathrm{e}^{-(b_1+b_2+b_3)D_\mathrm{T}}f(G',\delta',n)\sum_{m=-\infty}^{\infty}\mathrm{i}^m\mathrm{J}_m\left(\xi\right)\left[\left(\mathrm{e}^{\mathrm{i}(n+m+1)\phi_{z1}}-\mathrm{e}^{\mathrm{i}(n+m-1)\phi_{z1}}\right)\right].\tag{11}$$

Since ϕ_{z1} is much larger than 2π, averaging over the sample causes the signal to vanish unless $m=-n\pm1$. So Eq.(11) can be simplified to

$$M_+(\tau,t_2)=\frac{M_0}{2}\mathrm{i}^{-n-1}\mathrm{e}^{-(\tau+t_2)/T_2}\mathrm{e}^{-(b_1+b_2+b_3)D_\mathrm{T}}f(G',\delta',n)$$
$$\times\left[\mathrm{J}_{-n-1}\left(\xi\right)+\mathrm{J}_{-n+1}\left(\xi\right)\right].\tag{12}$$

According to the properties of the Bessel function, the resulting signal can then be written as

$$M_+(\tau,t_2)=\mathrm{i}^{n-1}M_0n\frac{\mathrm{J}_n\left(-\xi\right)}{\xi}\mathrm{e}^{-(\tau+t_2)/T_2}\mathrm{e}^{-(b_1+b_2+b_3)D_\mathrm{T}}f(G',\delta',n).\tag{13}$$

In order to make the formalism tractable, we limit it to the cases with $\xi\ll1$, i.e. with weak DDF effects. This requirement is safely fulfilled under ordinary experimental conditions. In such cases, all the terms except the first-order one in the Taylor series expansion for the Bessel function can be neglected. For $n=2$, Eq.(13) can be written as

$$M_+^{\mathrm{iDQC}}(\tau,t_2)=\frac{\mathrm{i}\,\gamma\mu_0M_0^2\mathrm{e}^{-\tau/T_2}\mathrm{e}^{-b_1D_\mathrm{T}}\left[1-\mathrm{e}^{-\left(k^2D_\mathrm{T}+1/T_1\right)t_2}\right]}{4\left(k^2D_\mathrm{T}+1/T_1\right)}$$
$$\times\mathrm{e}^{-(t_2+\tau)/T_2}\mathrm{e}^{-(b_1+b_2+b_3)D_\mathrm{T}}\mathrm{e}^{-k^2t_2D_\mathrm{T}}\mathrm{e}^{-\left(2\gamma G'\delta'\right)^2\left(\delta'/3+t_2\right)D_\mathrm{T}}.\tag{14}$$

Here the diffusion effects contribute in two ways. On one hand, the molecular displacements during the mixing period attenuate the signal amplitude in the conventional way. On the other hand, additional diffusion attenuation is expected due to the presence of DFG. After Fourier transformation, the signal intensity in the frequency domain for acquisition time T can be represented as follows:

$$I=\int_0^T M_+^{\mathrm{iDQC}}(\tau,t_2)\mathrm{d}t_2.\tag{15}$$

Substituting Eq.(14) into Eq.(15), we obtain the relative signal attenuation factor E for iDQCs in the frequency domain:

$$E=\frac{\int_0^T M_+^{\mathrm{iDQC}}(\tau,t_2)_G\mathrm{d}t_2}{\int_0^T M_+^{\mathrm{iDQC}}(\tau,t_2)_{G_{\min}}\mathrm{d}t_2}.\tag{16}$$

2.2. The diffusion effect in the pre-acquisition period

In this subsection, we will discuss the diffusion attenuation due to the DFG and DWGs in the pre-acquisition period. For unrestricted isotropic diffusion, the diffusion weighting factor b in this period

can be defined as[34,35]

$$b = b_2 + b_3 = \gamma^2 \int_{\tau}^{\tau+\delta'+\Delta+\delta} \left(\int_0^{t'} \boldsymbol{G}(t_2)\mathrm{d}t_2 \right)^2 \mathrm{d}t' = b_x + b_y + b_z, \tag{17}$$

where b_x, b_y and b_z are x, y and z components of b, respectively. Let $\boldsymbol{F}(t')$ be the time integration of gradient

$$\boldsymbol{F}(t') = \int_0^{t'} \boldsymbol{G}(t_2)\mathrm{d}t_2. \tag{18}$$

For simplicity, we only studied two special cases: $\boldsymbol{G}$ is perpendicular to the z direction, and $\boldsymbol{G}$ is parallel ($\theta = \pi/2$) or anti-parallel ($\theta = -\pi/2$) to the z direction. In the following calculations, G_d is the amplitude of the effective DFG generated by the DDF and is defined by Eq.(8).

When $\theta = \pi/2$, all the gradients are along the z direction, so the integral of gradient function is

$$F(t') = \begin{cases} G_{\mathrm{d}}t', & \tau < t' \le \tau + \delta', \\ G_{\mathrm{d}}t' + G\left(t' - \tau - \delta'\right), & \tau + \delta' < t' \le \tau + \delta' + \delta, \\ G_{\mathrm{d}}t' + G\delta, & \tau + \delta' + \delta < t' \le \tau + \delta' + \Delta, \\ G_{\mathrm{d}}t' + G\delta - G\left(t' - \tau - \delta' - \Delta\right), & \tau + \delta' + \Delta < t' \le \tau + \delta' + \Delta + \delta. \end{cases} \tag{19}$$

When $\theta = -\pi/2$,

$$F(t') = \begin{cases} G_{\mathrm{d}}t', & \tau < t' \le \tau + \delta', \\ G_{\mathrm{d}}t' - G\left(t' - \tau - \delta'\right), & \tau + \delta' < t' \le \tau + \delta' + \delta, \\ G_{\mathrm{d}}t' - G\delta, & \tau + \delta' + \delta < t' \le \tau + \delta' + \Delta, \\ G_{\mathrm{d}}t' - G\delta + G\left(t' - \tau - \delta' - \Delta\right), & \tau + \delta' + \Delta < t' \le \tau + \delta' + \Delta + \delta. \end{cases} \tag{20}$$

Both $\boldsymbol{F}(t')$ are along the z direction. So the b value can be calculated as follows:

$$b = \begin{cases} \gamma^2 G_{\mathrm{d}}^2 (\delta' + \Delta + \delta)^3/3 + \gamma^2 G^2 \delta^2 (\Delta - \delta/3) + \gamma^2 G_{\mathrm{d}} G \Delta\delta (\delta' + \Delta + \delta), & (\theta = \pi/2), \\ \gamma^2 G_{\mathrm{d}}^2 (\delta' + \Delta + \delta)^3/3 + \gamma^2 G^2 \delta^2 (\Delta - \delta/3) - \gamma^2 G_{\mathrm{d}} G \Delta\delta (\delta' + \Delta + \delta), & (\theta = -\pi/2). \end{cases} \tag{21}$$

The b values caused by the DWGs and DFG can then be expressed as

$$\begin{cases} b_2 = \gamma^2 G^2 \delta^2 (\Delta - \delta/3), \\ b_3 = \gamma^2 G_{\mathrm{d}}^2 (\delta' + \Delta + \delta)^3/3 \pm \gamma^2 G_{\mathrm{d}} G \Delta\delta (\delta' + \Delta + \delta), \end{cases} \tag{22}$$

in which $b^{\mathrm{ct}} = \pm\gamma^2 G_{\mathrm{d}} G \Delta\delta (\delta' + \Delta + \delta)$ is a term arising from the coupling between DWGs and DFG.

When the direction of gradient G is along the x direction ($\theta = 0$ or π), the diffusion weighting factor can be deduced

$$b_x = \gamma^2 G^2 \delta^2 (\Delta - \delta/3). \tag{23}$$

Since the DFG is along the z direction, we have

$$b_z = \gamma^2 G_{\mathrm{d}}^2 (\delta' + \Delta + \delta)^3/3. \tag{24}$$

So the total b value is

$$b = \gamma^2 G^2 \delta^2 (\Delta - \delta/3) + \gamma^2 G_{\mathrm{d}}^2 (\delta' + \Delta + \delta)^3/3. \tag{25}$$

Therefore, we have

$$\begin{cases} b_2 = \gamma^2 G^2 \delta^2 (\Delta - \delta/3), \\ b_3 = \gamma^2 G_{\mathrm{d}}^2 (\delta' + \Delta + \delta)^3/3. \end{cases} \tag{26}$$

According to the above deduction, the diffusion weighting factor b in the pre-acquisition period can be summarized as follows:

$$\begin{cases} b = \gamma^2 G_{\rm d}^2(\delta' + \Delta + \delta)^3/3 + \gamma^2 G^2\delta^2\left(\Delta - \delta/3\right) + \gamma^2 G_{\rm d} G\Delta\delta\left(\delta' + \Delta + \delta\right), & (\theta = \pi/2)\,, \\ b = \gamma^2 G_{\rm d}^2(\delta' + \Delta + \delta)^3/3 + \gamma^2 G^2\delta^2\left(\Delta - \delta/3\right) - \gamma^2 G_{\rm d} G\Delta\delta\left(\delta' + \Delta + \delta\right), & (\theta = -\pi/2)\,, \\ b = \gamma^2 G^2\delta^2\left(\Delta - \delta/3\right) + \gamma^2 G_{\rm d}^2(\delta' + \Delta + \delta)^3/3, & (\theta = 0 \text{ or } \pi)\,. \end{cases} \tag{27}$$

It is shown that coupling between the DWGs and the DFG occurs when the DWGs are along the $\pm z$ direction, i.e. parallel or anti-parallel to the direction of DFG. In such cases the diffusion attenuation due to the DFG varies with G. On the other hand, when the DWG is along the x direction, i.e. perpendicular to the DFG, the diffusion attenuation due to the DFG is independent of G. If all parameters in Eq.(27) are held constant except G, substituting Eqs.(14) and (27) into Eq.(16), we have

$$E = {\rm e}^{-\gamma^2\left[\delta^2(\Delta-\delta/3)G^2 + G_{\rm d}\Delta\delta\left(\delta'+\Delta+\delta\right)G\right]D_{\rm T}}, \quad (\theta = \pi/2)\,, \tag{28a}$$

$$E = {\rm e}^{-\gamma^2\left[\delta^2(\Delta-\delta/3)G^2 - G_{\rm d}\Delta\delta\left(\delta'+\Delta+\delta\right)G\right]D_{\rm T}}, \quad (\theta = -\pi/2)\,, \tag{28b}$$

$$E = {\rm e}^{-\gamma^2\delta^2(\Delta-\delta/3)G^2 D_{\rm T}}, \quad (\theta = 0 \text{ or } \pi)\,. \tag{28c}$$

For Eq.(28c), the natural logarithm of the signal intensity is linearly related to G^2. The slope of the line of $\ln E$ versus G^2 is proportional to the conventional molecular translational diffusion coefficient $D_{\rm T}$. However, in Eqs.(28a) and (28b), the natural logarithm of the signal intensity is nonlinear versus G^2 since the diffusion is modulated by the coupling between the DFG and DWGs. Using Eq.(28), we can gain the diffusion coefficient $D_{\rm T}$ by fitting the result to the experimental curve of $\ln E$ versus G.

According to the literature, the relationship between $\ln E$ and G^2 for conventional SQCs is $E = {\rm e}^{-\gamma^2\delta^2(\Delta-\delta/3)G^2 D_{\rm T}}$,[7] the same as Eq.(28c). So we can obtain the diffusion modulation factor for iDQCs from Eq.(28)

$$\eta_{\rm mod} = 1 + \frac{G_{\rm d}\Delta\left(\delta' + \Delta + \delta\right)}{\delta\left(\Delta - \delta/3\right)G}, \quad (\theta = \pi/2)\,, \tag{29a}$$

$$\eta_{\rm mod} = 1 - \frac{G_{\rm d}\Delta\left(\delta' + \Delta + \delta\right)}{\delta\left(\Delta - \delta/3\right)G}, \quad (\theta = -\pi/2)\,, \tag{29b}$$

$$\eta_{\rm mod} = 1, \quad (\theta = 0 \text{ or } \pi)\,. \tag{29c}$$

From the above equations, the apparent diffusion coefficients of iDQCs during pre-acquisition can then be given as

$$D_{\rm iDQC}^{\rm app} = D_{\rm T}\eta_{\rm mod}. \tag{30}$$

Equations (29) and (30) show that apparent diffusion coefficient of iDQCs during the pre-acquistion period is a function of DFG (determined by CSG) and DWG when the directions of these gradients are parallel or anti-parallel to each other, and it will approach the conventional SQC diffusion coefficient when the CSG is close to zero.

3. Materials and methods

All experiments were carried out on a Varian NMR System 500 MHz spectrometer equipped with a 5 mm actively shielded x, y, z axis gradient indirect detect probe. Gradient strengths were calibrated with gradient profile experiments. The pulse sequence shown in Fig.1 was used to measure the iDQC signals. The diffusion weighted module is a pair of gradients with opposite polarity. For conventional SQC signals, the pulse sequence was a $\pi/2$ RF pulse followed by a diffusion weighting module along the x direction before acquisition. The sample was a mixture of 80% acetone and 20% acetone-d_6. All ^{1}H NMR spectra were recorded at 298 K. To suppress the effects of radiation damping, the width of the $\pi/2$ RF pulse was extended to 95.5 μs by deliberately detuning the probe. A typical set of experimental parameters were as follows: a relaxation delay (RD) of 30 s, to recover the magnetization to its full equilibrium state and prevent any possible stimulated echoes; acquisition time 2.0 s; G' was varied in order to obtain different DFG and the duration $\delta' = 2$ ms; $\tau = 2.5$ ms; $\Delta = 14$ ms. G was varied along the z ($\theta = \pi/2$), $-z$ ($\theta = -\pi/2$) and x ($\theta = 0$) directions to produce a series of diffusion weighting, and $\delta = 4$ ms. Theoretical simulations were performed to verify the experimental observations.[29] The simulation parameters were set to the same as the experimental ones and the relaxation times were $T_1 = 5$ s and $T_2 = 2$ s. The effects of radiation damping were neglected.

To demonstrate that the observed signals are really from iDQCs and insensitive to the DWG direction, magic angle experiments were carried out with the DWG direction parallel ($\theta = \pi/2$ or $-\pi/2$) or perpendicular ($\theta = 0$) to the z direction.

4. Experimental results and discussion

The results of the magic angle experiments are presented in Fig.2. It shows that the signal intensity of the left ($\phi = 90°$) is about twice that of the right ($\phi = 0°$), but is very weak when the CSG direction is along the magic angle ($\phi = 35.3°$), indicating that the signal really comes from iDQCs, as expected theoretically.

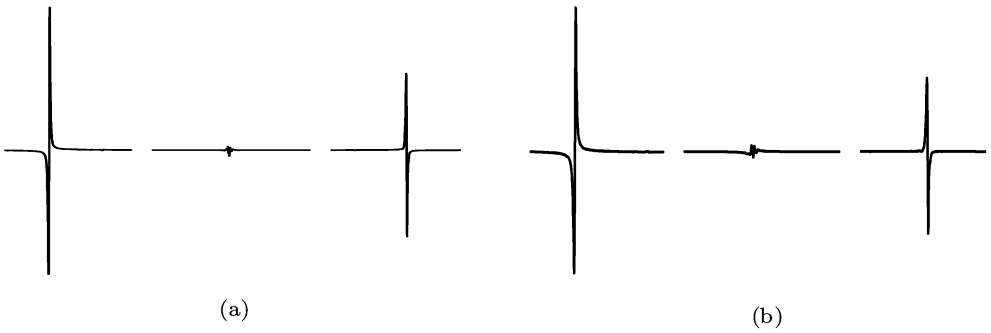
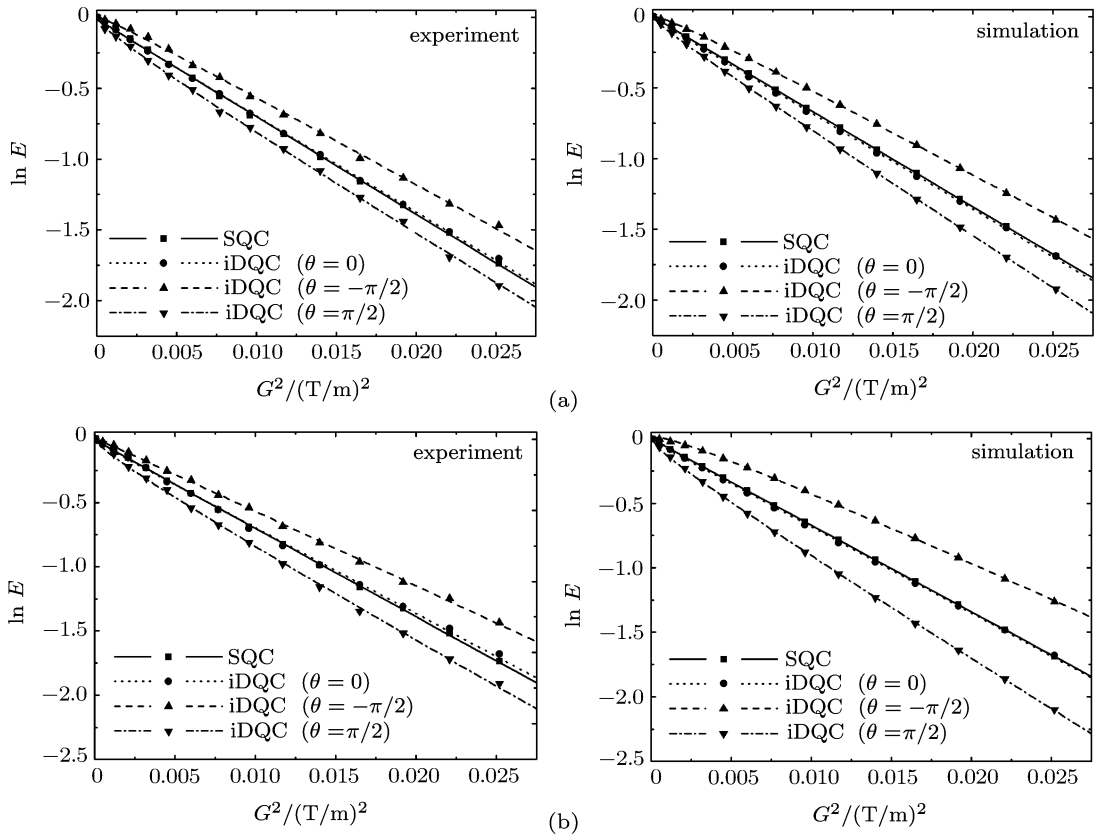


Fig.2. (a) Signals from the pulse sequence shown in Fig.1 with the DWGs parallel or anti-parallel to the z direction ($\theta = \pi/2$ or $-\pi/2$), and CSGs along $\phi = 90°$ (left), $\phi = 35.3°$ (middle), and $\phi = 0°$ (right). (b) Signals corresponding to (a) with the DWGs perpendicular to the z direction ($\theta = 0$).

To determine the diffusion coefficients under different DDF modulation, a series of ^{1}H iDQC and SQC spectra were measured with different amplitudes of CSGs and different amplitudes and directions of DWGs. For the diffusion coefficients under a specific DDF modulation, all experimental parameters were set to the same as above except the G value.



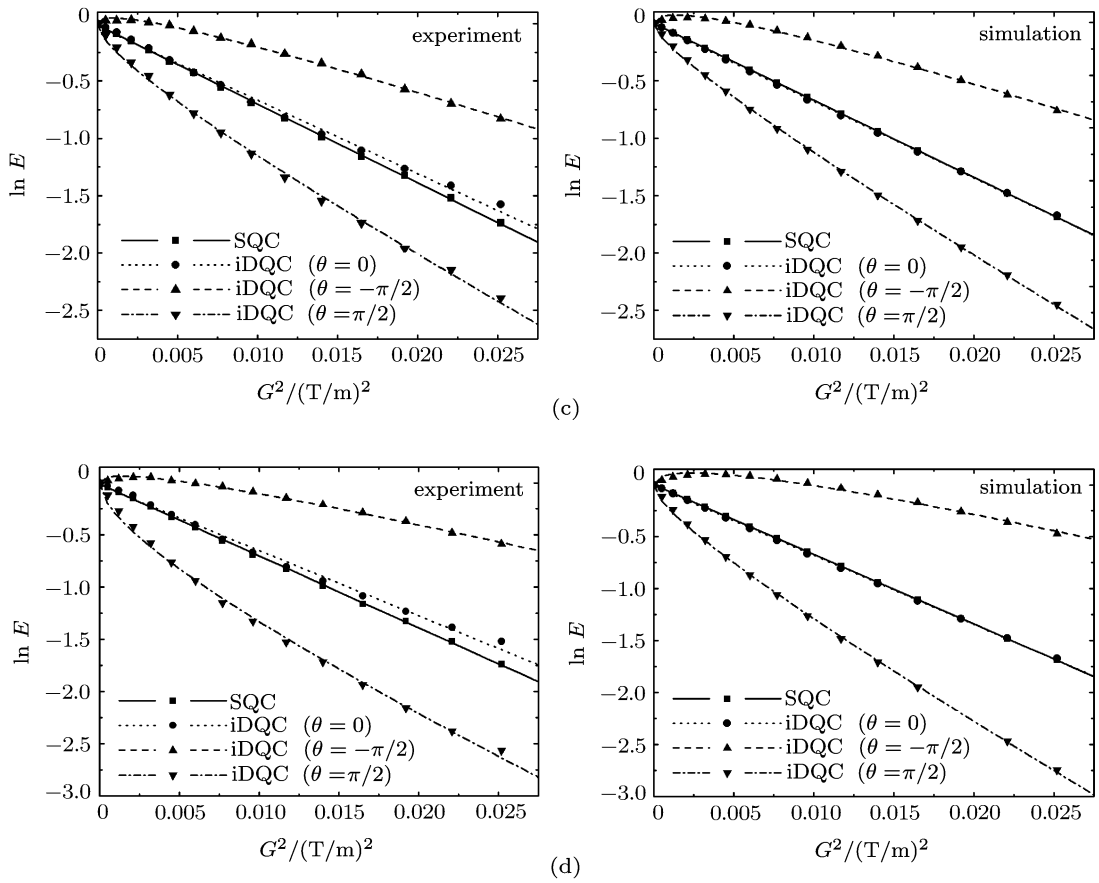


Fig.3. Experimental (left) and simulated (right) results of signal attenuation due to the diffusion of acetone molecules in the mixture of acetone and acetone-d_6 during the pre-acquisition period of the CRAZED sequence with $\phi = \pi/2$. (a) $G' = 20$ mT/m; (b) $G' = 40$ mT/m; (c) $G' = 100$ mT/m; (d) $G = 150$ mT/m. The symbols indicate the experimental or simulated data points, and the lines are fitting curves according to Eq.(28).

Plots of natural logarithms of the relative peak areas $\ln E$ versus G^2 with G' set to 20, 40, 100 and 150 mT/m, respectively, are shown in Fig.3. For conventional SQCs and iDQCs with the DWGs along the x direction ($\theta = 0$), since $\ln E = -\gamma^2\delta^2\,(\Delta - \delta/3)\,D_{\rm T}G^2$ and $\gamma^2\delta^2\,(\Delta - \delta/3)\,D_{\rm T}$ is constant, the relationship between $\ln E$ and G^2 is linear and the slope of $\ln E - G^2$ line is proportional to $D_{\rm T}$.

When the DWGs are parallel or anti-parallel to the z direction ($\theta = \pi/2$ or $-\pi/2$), the $\ln E - G^2$ curves are nonlinear for iDQCs. They deviate from the line of $\theta = 0$ to different directions. As shown in Eqs.(28)–(30), an additional diffusion modulation exists due to the coupling between the DFG and DWGs, and the signal attenuation is not constant when the DWG changes. When $\theta = \pi/2$, $b^{\rm ct}$ is positive, and the diffusion modulation factor $\eta_{\rm mod}^{\theta=\pi/2}$ increases with the increase of G' strength. In contrast, $b^{\rm ct}$ is negative when $\theta = -\pi/2$, thus $\eta_{\rm mod}^{\theta=-\pi/2}$ decreases when the G' strength increases. This is the reason why the $\ln E - G^2$ curves are nonlinear and deviate from the line of $\theta = 0$ to different directions, as shown in Fig.3. The stronger the G', the more serious the nonlinear effects. The diffusion coefficients $D_{\rm T}$ obtained by fitting the $\ln E - G^2$ curves with Eq.(27) are summarized in Table 1.

Table 1. Diffusion coefficients $D_{\rm T}$ ($\times 10^{-9}$ m^2/s) of acetone obtained under different conditions.

G'/(mT/m)	$D_{\rm T}^{\theta=\pi/2}$		$D_{\rm T}^{\theta=-\pi/2}$		$D_{\rm T}^{\theta=0}$		$D_{\rm T}^{\rm SQC}$	
	experiment	simulation	experiment	simulation	experiment	simulation	experiment	simulation
20	4.47±0.08	4.60±0.02	4.45±0.10	4.59±0.03	4.61±0.03	4.63±0.01	4.64±0.05	4.63±0.02
40	4.48±0.11	4.59±0.04	4.44±0.11	4.57±0.05	4.60±0.05	4.63±0.01		
100	4.48±0.19	4.58±0.09	4.43±0.07	4.56±0.08	4.56±0.07	4.62±0.02		
150	4.46±0.26	4.56±0.10	4.41±0.08	4.56±0.12	4.49±0.08	4.62±0.02		

When $\theta = 0$ or π, the directions of DWGs and DFG are perpendicular to each other. There is no coupling term in Eq.(28c). Therefore, the influence of DDF on signal attenuation is kept constant at various diffusion weightings, resulting in a linear relationship of $\ln E - G^2$. According to the theoretical formula, under this situation the apparent diffusion coefficient $D_{\mathrm{T}}^{\theta=0}$ should be invariable and equal to $D_{\mathrm{T}}^{\mathrm{SQC}}$ even if the amplitude of CSGs is changed. This is the case for simulation results. However, as shown in Table 1, the experimental $D_{\mathrm{T}}^{\theta=0}$ varies slightly with the increase of CSG strength. This may be due to the spatial distribution of the gradients in the practical experiments. Since DWGs and DFG are along the x and z directions respectively, the effective DWG amplitude in Eq. (30) should be $G_{\mathrm{eff}} = \sqrt{G_x^2 + G_z^2}$, where $G_x = G$, $G_z = G_{\mathrm{d}}$. When G' is small, G_{d} is much smaller than G. So $G_{\mathrm{eff}} \approx \sqrt{G_x^2} = G$, and the effective DWG is along the $\pm x$ direction. In other words, the diffusion in the x direction is hardly affected by G_{d}. However, with the increase of G', G_{d} increases too, thus the effective DWG is no longer strictly along the $\pm x$ direction, but has a slight deviation. Consequently, the experimental curve of $\theta = 0$ in Fig.3 deviates from the SQC one and is close to the curve of $\theta = \pi/2$. The diffusion coefficient $D_{\mathrm{T}}^{\theta=0}$ changes accordingly and becomes closer to the values of $D_{\mathrm{T}}^{\theta=\pi/2}$ with the increase of G' strength. Since the largest deviation of experimental $D_{\mathrm{T}}^{\theta=0}$ from D_{T} is only about 3%, the effect of G_{d} can be neglected, and the diffusion of iDQCs when $\theta = 0$ or π can be taken to be still governed by Eq.(28c). In simulations, such an effect was not taken into account, thus the resulting $D_{\mathrm{T}}^{\theta=0}$ values at various G' are very close to each other.

When $\theta = \pi/2$ or $-\pi/2$, the experimental results of $D_{\mathrm{T}}^{\theta=\pm\pi/2}$ agree well with each other, as do the simulated $D_{\mathrm{T}}^{\theta=\pm\pi/2}$ values. Both experimental and simulated $D_{\mathrm{T}}^{\theta=\pm\pi/2}$ deviate slightly from their corresponding $D_{\mathrm{T}}^{\mathrm{SQC}}$. The simulated results are much closer to $D_{\mathrm{T}}^{\mathrm{SQC}}$. The largest deviations are smaller than 5% and 2% for the experimental and simulation results respectively. The deviations from $D_{\mathrm{T}}^{\mathrm{SQC}}$ may be mainly due to the complex coupling effect between the DFG and DWGs. Since the errors in nonlinear fittings are generally greater than those in linear fittings, these deviations are acceptable. On the other hand, the deviations between experimental and simulated results may come from overlooking some influencial factors during simulation. In simulation, we only considered ideal unrestricted isotropic diffusion and factors like sample shape and radiation damping; background field inhomogeneity was completely ignored. However, in practical CRAZED experiments, these factors might have an influence on the signal intensity.

5. Conclusion

In this paper, a modified CRAZED sequence was designed to study the apparent diffusion behaviour of iDQCs in the pre-acquisition period. Theoretical formulas were derived from the dipolar field model. Experiments and simulations were performed to verify the theoretical predictions. The results show that the iDQC apparent diffusion behaviour in the pre-acquisition period is related to the orientation of DWGs relative to that of CSGs. When these two directions are parallel or anti-parallel to each other, the diffusion can be modulated by the DDF and the apparent diffusion coefficient increases or decreases with the change of the direction of DWGs relative to that of CSGs; when the orientation of DWGs is perpendicular to that of CSGs, the diffusion is not affected by the DDF.

References

[1] Bowtell R, Bowley R M and Glover P 1990 *J. Magn. Reson.* **88** 643

[2] Warren W S, Richter W, Andreotti A H and Farmer II B T 1993 *Science* **262** 2005

[3] Kimmich R and Ardelean I 1999 *J. Chem. Phys.* **110** 3708

[4] Jeener J 1999 *Phys. Rev. Lett.* **82** 1772

[5] Chen S, Zhu X Q, Cai S H and Chen Z 2008 *Chin. Phys.* B **17** 915

[6] Zhang L, Liu Z, Chen Q and Hansen E W 2007 *Macromolecules* **40** 5411

[7] Chen Z and Zhong J H 2001 *J. Chem. Phys.* **114** 5642

[8] Shannon K L, Branca R T, Galiana G, Cenzano S, Bouchard L S, Soboyejo W and Warren W S 2004 *Magn. Reson. Imaging* **22** 1407

[9] Zheng B W, Hwang D W, Chen Z and Hwang L P 2005 *Magn. Reson. Med.* **53** 930

[10] Zhu X Q, Cai C B, Chen Z and Zhong J H 2005 *Chin. Phys.* **14** 516

[11] Peng M and Chen Q 2008 *Chem. Phys. Lett.* **456** 189

[12] Cai C B, Lin Y Q, Cai S H, Chen Z and Zhong J H 2008 *J. Magn. Reson.* **193** 94

[13] Cui X H, Mao S Z, Liu M L, Yuan H Z and Du Y R 2008 *Langmuir* **24** 10771

[14] Warren W S, Ahn S, Mescher M, Garwood M, Ugurbil K, Richter W, Rizi R R, Hopkins J and Leigh J S 1998 *Science* **281** 247

[15] Roth Y, Ocherashvilli A, Daniels D, Ruiz-Cabello J, Maier S E, Orenstein A and Mardor Y 2008 *Magn. Reson. Imaging* **26** 88

[16] Faber C, Heil C, Zahneisen B, Balla D Z and Bowtell R 2006 *J. Magn. Reson.* **182** 315
[17] Kaufmann I, Seiberlich N, Haase A and Jakob P 2008 *J. Magn. Reson.* **192** 139
[18] Navon G, Eliav U, Demo D E and Blumich B 2007 *J. Magn. Reson. Imaging* **25** 362
[19] Ababneh Z Q, Ababneh R, Maier S E, Winalski C S, Oshio K, Ababneh A M and Mulkern R V 2008 *Magn. Reson. Mat. Phys. Biol. Med.* **21** 273
[20] Fasano F, Capuani S, Hagberg G E, Branca T, Indovina I, Castriota-Scanderbeg A and Maraviglia B 2003 *Magn. Reson. Imaging* **21** 1151
[21] Schafer A and Moller H E 2007 *Magn. Reson. Med.* **58** 696
[22] Ardelean I, Kossel E and Kimmich R 2001 *J. Chem. Phys.* **114** 8520
[23] Chen L P, Gross T, Krienke H and Ludemann H D 2001 *Phys. Chem. Chem. Phys.* **3** 2025
[24] Liu A H, Mao S Z, Liu M L, Zhang Y X, Wu F P, Li M Z, Wang E J, Cheng G Z and Du Y R 2007 *Colloid Polym. Sci.* **285** 381
[25] Xu M, Zhang H P and Chen Q 2004 *Chem. J. Chin. Univ.-Chin.* **25** 1901
[26] Ozarslan E and Basser P J 2007 *J. Magn. Reson.* **188** 285
[27] Chen L P, Gross T and Ludemann H D 2001 *Chin. J. Chem.* **19** 453
[28] Gao H C, Mao S Z, Dai Y H, Li M Z, Yuan H Z, Wang E J and Du Y R 2005 *Colloid Polym. Sci.* **283** 496
[29] Cai C B, Lin M J, Chen Z, Chen X, Cai S H and Zhong J H 2008 *C. R. Phys.* **9** 119
[30] Sklenar V 1995 *J. Magn. Reson.* A **114** 132
[31] Garrett-Roe S and Warren W S 2000 *J. Magn. Reson.* **146** 1
[32] Lee S, Richter W, Vathyam S and Warren W S 1996 *J. Chem. Phys.* **105** 874
[33] Levitt M 1996 *Concepts Magn. Reson.* **8** 77
[34] Setjskal E O and Tanner J E 1965 *J. Chem. Phys.* **42** 288
[35] Farrell J A D, Smith S A, Gordon-Lipkin E M, Reich D S, Calabresi P A and van Zijl P C M 2008 *Magn. Reson. Med.* **59** 1079